NUCLEAR SCIENCE AND TECHNIQUES **25**, 020101 (2014)

Design and study of a C-band pulse compressor for the SXFEL linac

WANG Chao-Peng (王超鹏),[1,2] FANG Wen-Cheng (方文程),[1]
TONG De-Chun (童德春),[3] GU Qiang (顾强),[1] and ZHAO Zhen-Tang (赵振堂)[1,*]

[1]*Shanghai Institute of Applied Physics, Chinese Academy of Sciences, Shanghai 201800, China*
[2]*University of Chinese Academy of Sciences, Beijing 100039, China*
[3]*Department of Engineering Physics, Tsinghua University, Beijing 100084, China*

(Received February 19, 2013; accepted in revised form March 22, 2014; published online April 20, 2014)

A C-band RF pulse compressor is in development at SINAP. It comprises of two resonant cavities, two mode convertors and a 3 dB power divider. $TE_{0.1.15}$ mode is selected for obtaining higher quality factor Q_0 of the RF pulse compressor cavities, so that the power gain factor can be 3.2, which is supposed to multiply the RF power from 50 MW to 160 MW. In this paper, we report our work on C-band RF pulse compressor, namely the design simulation and cold test results.

Keywords: C-band, Pulse compressor, High quality factor, High RF power

DOI: 10.13538/j.1001-8042/nst.25.020101

I. INTRODUCTION

A compact Soft X-ray Free Electron Laser test facility (SXFEL) is now underway at Shanghai Institute of Applied Physics (SINAP), Chinese Academy of Science. It will be neighboring the Shanghai Synchrotron Radiation Facility (SSRF), the first third generation light source in China. To make SXFEL even more compact, the third section of linac shall be composed of four C-band microwave acceleration units, with a high acceleration gradient of 40 MV/m [1]. This shall be realized by using a C-band RF pulse compressor, a crucial component for the C-band high gradient acceleration system. It will be tested together with the C-band accelerating structure in the SXFEL facility.

RF pulse compression is used to multiply RF power for increasing acceleration gradient. At present, several types of RF pulse compressor have been utilized at different facilities all over the world. Since the successful efforts at Stanfors Linear Accelerator Center on the prototype of pulse compressor, the SLAC Energy Doubler (SLED) [2–4] on SLC, higher efficiency and flat-top technology has been in rapid development for RF pulse compressors, such as SLED-II [5], small delay line RF pulse compressor [6, 7] (using coupled cavities), BPC [8], DLDS [9] and BOC [10]. As a compact FEL facility, SXFEL uses high efficiency, high gradient C band acceleration unit. RF pulse compressor with flat-top output pulse is the compromised proposal for both high efficiency and high accelerating gradient, which can be carried out by SLED-I controlled by AM-PM LLRF (low-level RF) modulation technology.

The proposed SLED-I comprises of two cavities, two mode convertors and a 3 dB power divider. $TE_{0.1.15}$ mode of the circular cavity is selected for higher quality factor of 180 000, and the power gain factor is targeted at 3.2. The 3 dB power divider, optimized for higher power-transmitting, is effective to avoid breakdown problems. A four-ports mode convertor is used to connect the 3 dB divider and resonant cavities, so that it can obtain more purity of TE01 mode than that of one-port or two-ports convertor, and so that only $TE_{0.1.15}$ mode exists for high quality factor.

In this paper, we present the design study of the C-band RF pulse compressor, with results of RF simulation and cold test of the resonant cavity.

II. CONFIGURATION AND PRINCIPLE OF RF PULSE COMPRESSOR

The C-band RF pulse compressor used for the C-band microwave acceleration unit of SXFEL is driven by a 50 MW klystron, as shown in Fig. 1. The RF pulses are compressed into shorter pulses. The RF power is thus increased by several times and divided into equal two parts for the two accelerating structures.

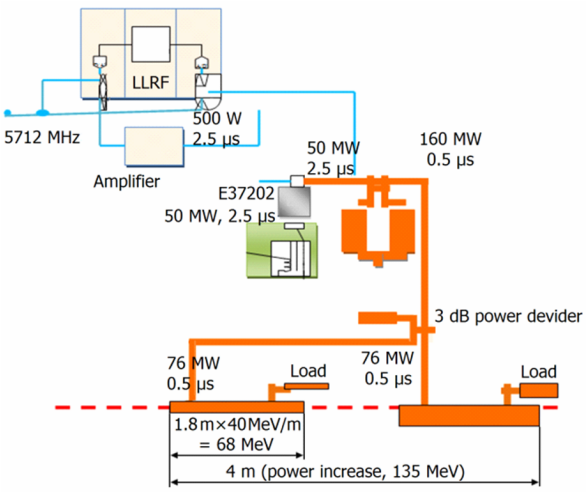

Fig. 1. (Color online) The sketch of C-band microwave acceleration unit of SXFEL.

The C-band accelerating structure of the SXFEL test facility is required to operate at the gradient of 40 MV/m. Cor-

* Corresponding author, zhaozt@sinap.ac.cn

respondingly, the input power for each acceleration structure should be 70 MW. Then, the klystron output power of 50 MW shall be enhanced to 160 MW by the RF pulse compressor. After waveguide dissipation, there will be 75 MW for each acceleration structure. Considering the design and fabrication, SLED-I is one compromised option. As shown in Fig. 2, it is composed of two identical high Q-value cavities, two mode convertors and a 3 dB power divider. Its performance depends on the resonant cavities.

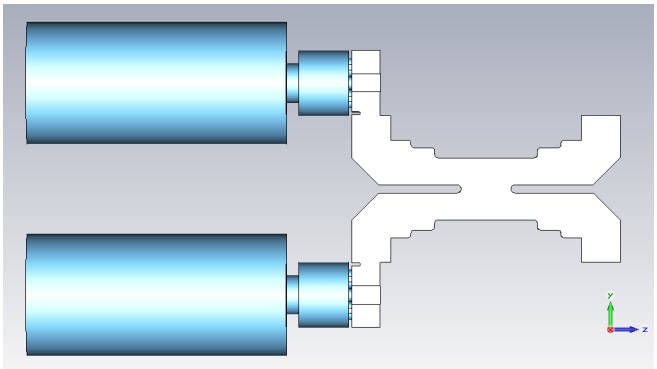

Fig. 2. (Color online) Schematic of the SLED type pulse compression.

In the C-band microwave unit, the klystron outputs RF pulses of 2.5 μs in width, and the power pulses are transmitted into the two SLED cavities. When electromagnetic field is induced in the cavities, waves of increasing amplitude are emitted from the coupling holes of two resonant cavities. Two emitted waves of the same phase are combined at the accelerator-side port of the 3 dB power divider, but are cancelled by 180° phase difference at the klystron-side port. There are two waves reflected from the coupling hole of the cavity, and waves emitted from inner cavity. The reflected and emitted waves are of 180° difference in phase, but they add together when the input wave is reversed to the same phase at the time of 2.0 μs.

From this principle of SLED-I, the power for the resonant cavity is expressed by Eq. (1):

$$T_{\rm c}{\rm d}E_{\rm e}/{\rm d}t + E_{\rm e} = -\alpha E_{\rm K}, \tag{1}$$

where, $\alpha = 2\beta/(1+\beta)$, β is the coupling coefficient; $T_{\rm c} = 2Q_{\rm L}/\omega$ is cavity filling time, Q_L is cavity load quality factor, ω is radian frequency; $E_{\rm e}$ is the emitted wave from the coupling aperture, and $E_{\rm K}$ is the reverse wave of equal magnitude to the incident wave. Considering the principle of SLED operation, Eq. (2) is derived as [2]:

$$\begin{aligned} E_{\rm L}(A) &= -\alpha e^{-\tau} + (\alpha - 1) && 0 \le t \le 2.0\,\mu{\rm s}, \\ E_{\rm L}(B) &= \gamma e^{-(\tau-\tau_1)} - (\alpha - 1) && 2.0\,\mu{\rm s} \le t \le 2.5\,\mu{\rm s}, \\ E_{\rm L}(C) &= \left[\gamma e^{-(\tau_2-\tau_1)} - \alpha\right] e^{-(\tau-\tau_1)} && t \ge 2.5\,\mu{\rm s}, \end{aligned} \tag{2}$$

where $\gamma \equiv \alpha(2 - e^{-\tau})$, $\tau = t/T_{\rm c}$, $\tau_1 = 2.0\,\mu$s and $\tau_2 = 2.5\,\mu$s. Fig. 3 shows the profiles of input wave and output wave of SLED. Although the energy gain factor is 2.5 in principle, as the LLRF system has power loss for modulation of flat-top output pulse, the final energy multiplication factor is about 1.8, and correspondingly, the power gain factor is 3.2.

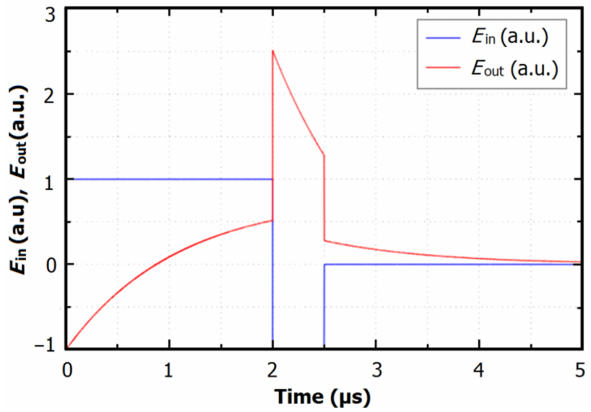

Fig. 3. (Color online) The profiles of input power and output power.

III. SIMULATION AND RESULTS

Based on theoretical analysis, MATLAB is used for parameters optimization of the Q-value, coupling coefficient and power efficiency. CST MICROWAVE STUDIO [11], which is good at asymmetrical structure computation, is used for three-dimensional electromagnetic simulation.

A. Resonant cavity

As a crucial component for an RF pulse compressor, a resonant cavity stores the energy and dominates performance of the RF pulse compressor, such as the gain factor and power efficiency. By tuning the Q_0 and the coupling coefficient, the RF power efficiency and energy multiplication factor can be mapped, as shown in Fig. 4. The optimal parameters are decided by the practical applications. In our design, for a multiply factor of 3.2, the coupling coefficient is fixed at 8.5 and Q at 180 000.

$TE_{0.1.15}$ is used for higher quality factor, with lower power loss on the copper surface. However, there are many modes that are close to $TE_{0.1.15}$ and are harmful for SLED-I performance, hence the need of cavity geometry optimization to suppress those modes is proposed. The frequency of different modes can be expressed as Eq. (3) by cavity geometry parameters [12].

$$(f_0 D)^2 = 9\times 10^{20}[(\upsilon_{\rm mn}/\pi)^2 + (p/2)^2(D/l)^2], \tag{3}$$

where, f_0 is the $TE_{\rm m.n.p}/TM_{\rm m.n.p}$ frequency of the cavity, D is the cavity diameter, l is the cavity length. Using Eq. (3), $TE_{0.1.15}$ and its adjacent modes are given in Fig. 5, where each line indicates the relationship between the resonant frequency and the cavity parameters. The marked point is far

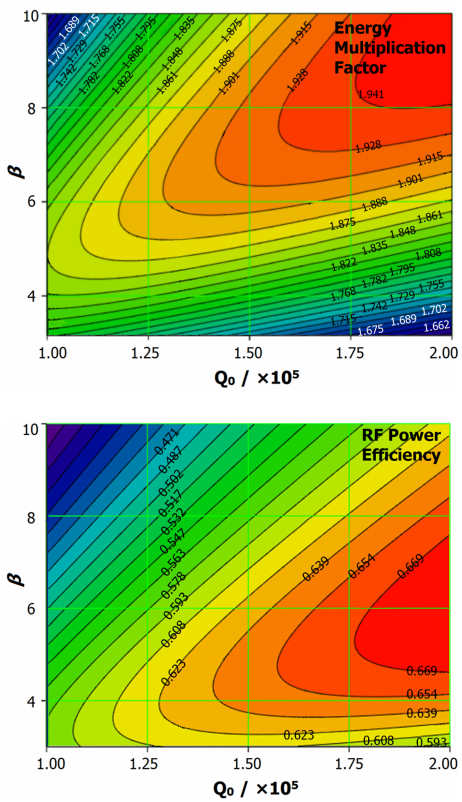

Fig. 4. (Color online) The multiplication factor and power efficiency mapped with the Q_0 and coupling coefficient.

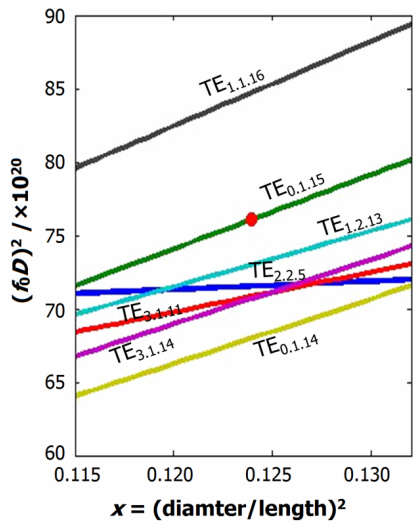

Fig. 5. (Color online) The mode chart of the circular cavity.

away from the adjacent modes, and the cavity geometry parameters are thus decided.

According to previous analysis, CST MICROWAVE STUDIO is used for three-dimensional field simulation, including frequency, Q_0 and coupling coefficient. The electromagnetic simulation results are shown in Fig. 6.

Based on the simulations, the frequency of resonant cavity

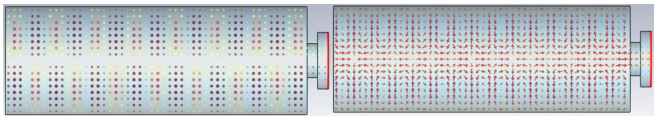

Fig. 6. (Color online) The electric (left) and magnetic (right) fields in the cavity of calculated by CST.

is fixed at 5712 MHz by adjusting the position of the end plat to find the exact coupling hole size for coupling coefficient of 8.5 and the final Q-value of the resonant cavity of about 180 000.

After the cavity fabrication, the operating frequency of $TE_{0.1.15}$ mode can be confirmed, so as to tune the cavity to 5712 MHz. As reference for measurements, we simulated the field distribution, Q-value and frequency sensitivities. Fig. 7 shows the simulated longitudinal magnetic field along the cavity axis and radius direction. For TE_{01} mode, the field distribution is axial symmetrical, magnetic field comprises of H_r and H_z component, but only E_φ exists for electrical field. There are 15 field peaks of H_z on axis based on the CST simulation (Fig. 7(a)) and the radial distribution of E_φ in the middle of the cavity (Fig. 7(b)).

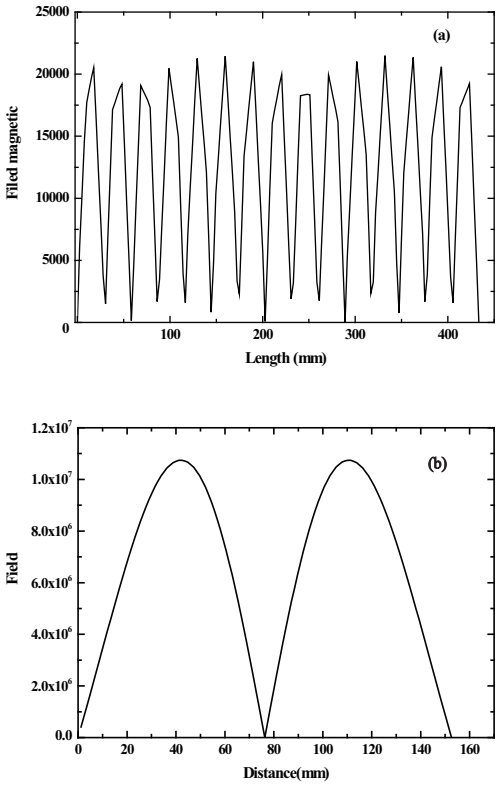

Fig. 7. Simulated longitudinal magnetic field along the cavity axis (a) and radius direction (b).

The frequency sensitivities against the cavity length and radius were calculated, too, as the reference for cavity tuning, with the frequency sensitivity of $\Delta f/\Delta l = 10.5$ MHz/mm for the cavity length (Fig. 8(a)) and $\Delta f/\Delta D = 6.6$ MHz/mm

for the cavity radius (Fig. 8(b)).

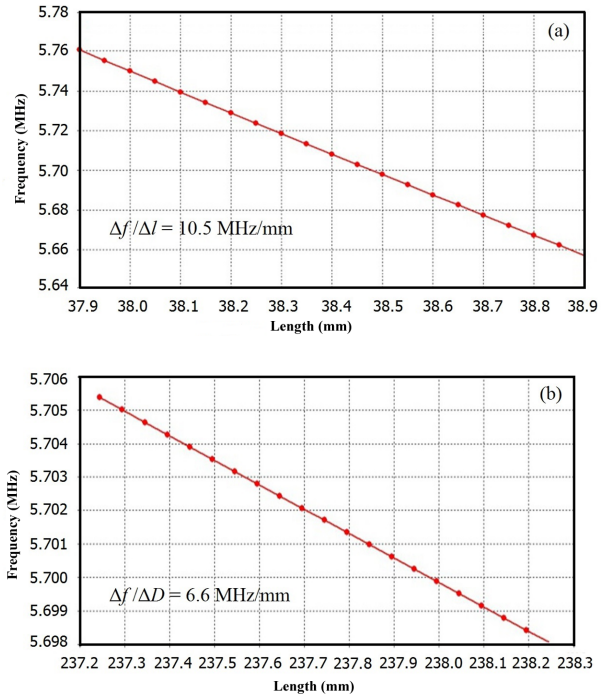

Fig. 8. (Color online) The frequency change with the cavity length (a) and the cavity radius (b).

B. 3 dB power divider

The 3 dB power divider is used to direct RF power into two cavities of the RF pulse compressor (Fig. 9). The power of the two cavities are added at the accelerator-side port and cancelled at the klystron-side port.

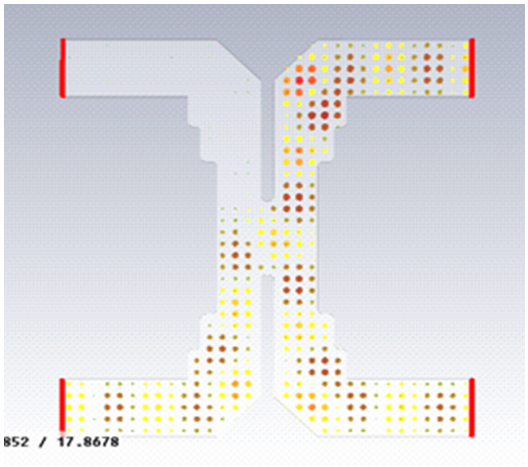

Fig. 9. (Color online) Simulation model of the 3-dB power divider.

Based on principle of the 3 dB power divider, the length L of coupling region can be tuned for matching, the input power can be equally divided into the two parts in Fig. 9. The analytical length L of matched status is expressed as Eq. (4), where λ_{g10} and λ_{g20} are the waveguide wavelength of the modes TE_{10} and TE_20 in the rectangular waveguide respectively [12].

$$\begin{aligned} L &= \frac{1}{4\left(\frac{1}{\lambda_{g10}}-\frac{1}{\lambda_{g20}}\right)}, \\ \lambda_{g10} &= \frac{\lambda}{\sqrt{1-\left(\frac{\lambda}{4a}\right)^2}}, \\ \lambda_{g20} &= \frac{\lambda}{\sqrt{1-\left(\frac{\lambda}{2a}\right)^2}}. \end{aligned} \tag{4}$$

Ladder type hybrid is used in the connection region for obtaining better performance and avoiding RF breakdown, while it is easier to input higher power. The CST simulation of the S-parameters of the 3 dB coupler divider is shown in Fig. 10, in which Port 1 is for the input power, Ports 2 and 3 are connected to two cavities, and Port 4 is used for the power output. From the figure, S11 and S41 are less than −30 dB, S21 and S31 are about −3 dB, reaching the design goal of power transmission and isolation.

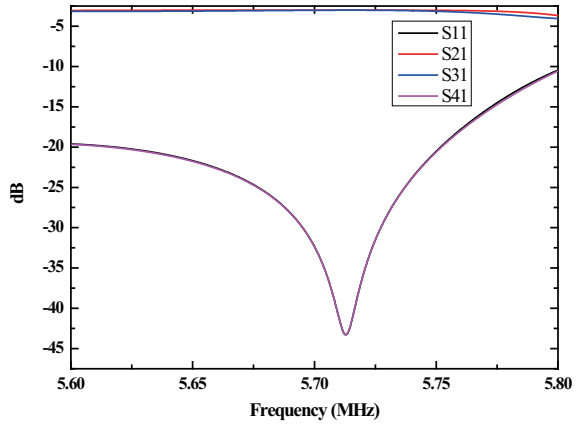

Fig. 10. (Color online) S-parameter of the 3 dB power divider by CST simulation.

C. Mode convertor

Mode convertor, located between the 3 dB power divider and resonant cavities, is used to obtain high purity of TE_{01} mode and convert TE_{10} of rectangular mode to TE_{01} of circular mode. Four coupling holes are designed for mode converter for stable operation at 80 MW (Fig. 11). Fig. 12 shows the simulated S-parameters for the mode converter. S21 and S11 are about 0 dB and −50 dB, respectively, well reaching the design goal.

Typical parameters of the C-band RF pulse compressor, comprising of two cavities, two mode convertors and a 3 dB power divider, are summarized in Table 1.

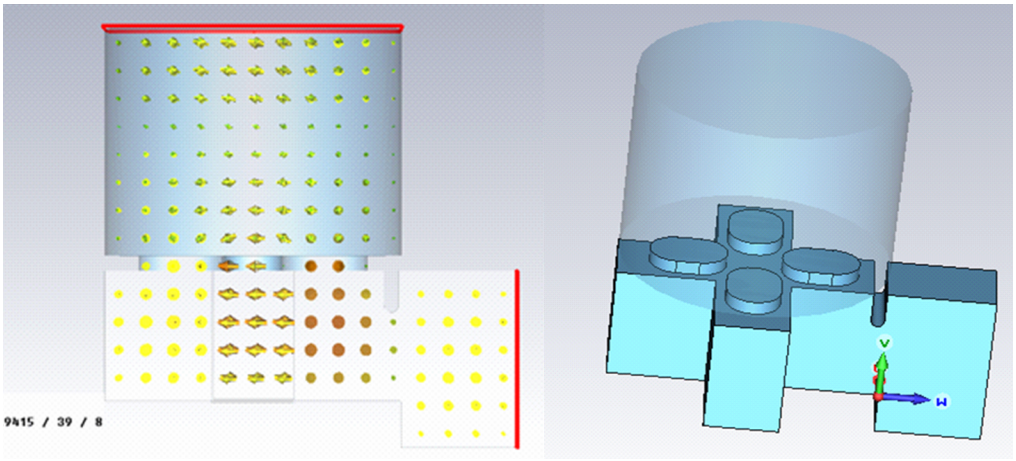

Fig. 11. (Color online) Schematics of the mode converter.

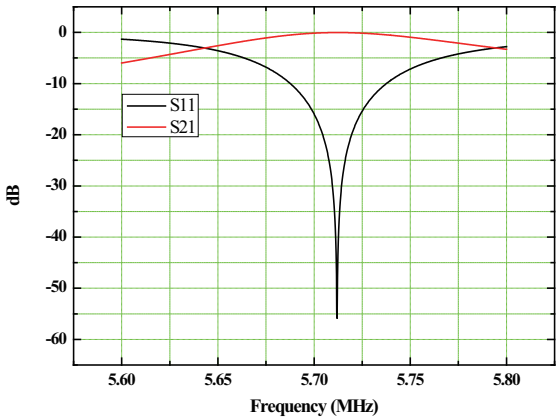

Fig. 12. (Color online) Schematics of the mode converter.

TABLE 1. Typical parameters of the C-band pulse compressor

Parameter	Value
Operation frequency	5712 MHz
Mode	$TE_{0.1.15}$
Quality factor	180 000
Power gain	3.2
Coupling coefficient	8.5

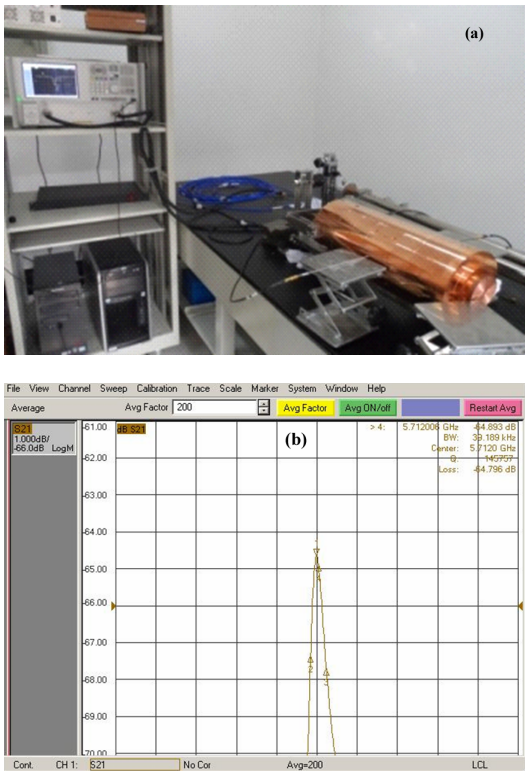

Fig. 13. (Color online) The measurement table of the C-band pulse compression cavity (a) and its Q-value and frequency measured (b).

IV. COLD TEST RESULTS OF RESONANT CAVITY

An experimental model of resonant cavity (Fig. 13(a)), with an input coupler, a tuner and a cavity, was fabricated to verify the design. The Q-value, frequency and field distribution along the axis were measured, and tuning experiments were carried out. As shown in Fig. 13(b), the measured frequency was 5711.63 MHz, and the Q-value was 159 640, a little lower than the design value, but this can be improved after brazing.

Longitudinal and radial distributions of H_z were measured by resonant perturbation (Fig. 14). The measured magnetic field distribution along the cavity axis (Fig. 14(a)), with 15 peaks, agrees well with the simulation result in Fig. 7(a), but the radial distribution (Fig. 14(b)) differs quite a little from the data in Fig. 7(b). This was caused by misalignment of measured line. In Fig. 7(b), the profile is located at the middle of cavity exactly; while in Fig. 14(b), the measured profile location was drifted by tuning process, so the test results consisted of both magnetic and electric fields.

The measured frequency sensitivity of cavity length is

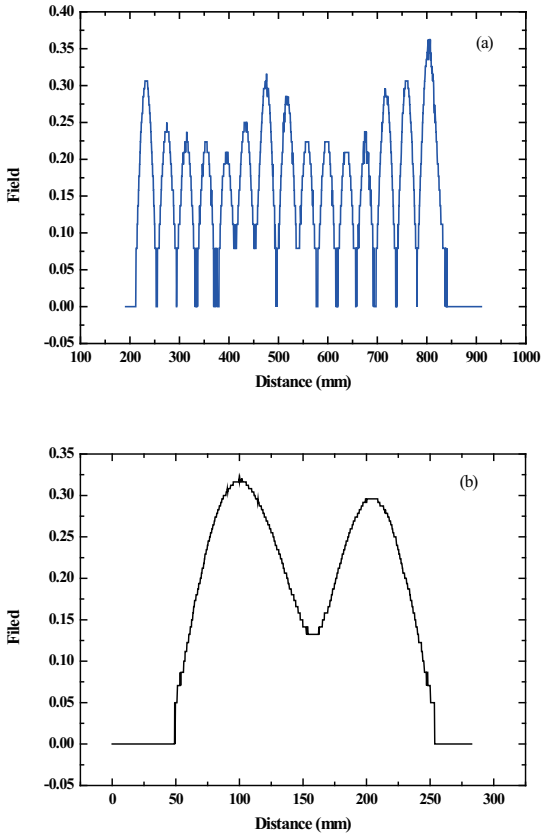

Fig. 14. (Color online) The measurement table of the C-band pulse compression cavity (a) and its Q-value and frequency measured.

$\Delta f/\Delta l = 10.5$ MHz/mm, agreeing well with the simulation data of $\Delta f/\Delta l = 10.4$ MHz/mm.

V. CONCLUSION

The C-band RF pulse compressor, as a crucial component for the SXFEL test facility, has been designed and simulated. A resonant cavity model was fabricated and tested under low RF power. To a large extent, the low power experiment results agree well with the design goals. This accumulates much data and experience for further development of the C-band RF pulse compressor. The experimental cavity design and mode measurement provide an integrated and systematic method for the R&D of C-band RF pulse compressor. The integral C-band RF pulse compressor will be fabricated, and high power RF tests will be processed soon.

ACKNOWLEDGMENTS

The authors are grateful to Dr. WANG Ju-Wen of the SLAC National Accelerator Laboratory for valuable suggestions and fruitful discussions. We would like to thank Professor CHEN Huai-Bi and coworkers at the Accelerator Laboratory of Tsinghua University for experiment supports.

[1] Fang W C, Gu Q, Tong D C, *et al*. Chinese Sci Bull, 2011, **56**: 3420–3425.
[2] Farkas Z D, Hogg H A, Loew G A, *et al*. SLED: A Method of Doubling SLAC's Energy, SLAC-PUB-1453, June 1974.
[3] Fiebig A, Schieblich Ch, Hogg G A, *et al*. A Radio Frequency Pulse Compressor for Square output Pulse, in Proc. EPAC88, Rome, Italy, June 7, 1988, pp.1075–1077.
[4] Farkas Z D, Hogg H A, Loew G A, *et al*. IEEE T Nucl Sci, 1975, **22**: 1299–1302.
[5] Wilson P B, Farkas Z D, Loew G A, *et al*. SLED II: A New Method of RF Pulse Compression, Linear Accelerator Conference, Albuquerque, NM, September 1990, SLAC-PUB-5330.
[6] Yoshida M. New concept samll delay line type pulse compressor using coupled cavities, in Proc. LINAC 2006, Tennessee, USA, August 20, 2006, pp. 667–669.
[7] Yoshida M. Ph.D. Thseis, The Research and Development of High Power C-band RF Pulse Compression System using Thermally Stable High-Q Cavity, 2003.
[8] Tantawi S G, Ruth R D, Vlieks A E, *et al*. Nucl Instrum Meth A, 1996, **370**: 297–302.
[9] Linac Coherent Light Source (LCLS) Conceptual Design Report, SLAC-R-593, April, 2002.
[10] Geschonke G and Ghigo A. CTF3 Design Report. CTF3 Note 2002-047 and LNF-02/008 (IR), CERN/PS 2002-008 (RF), 2002.
[11] www.cst.com
[12] Yan L R and Li Y H. Basis of microwave technique. Beijing Institute of Technology press, 2004, 308–310.